Indian Society for
Non-Destructive Testing
Hyderabad Chapter

Proc. National Seminar on
Non-Destructive Evaluation
Dec. 7 - 9, 2006, Hyderabad

3D Image Reconstruction from Truncated Helical Cone Beam Projection Data – A Linear Prediction Approach

K. Rajgopal and K.P. Anoop
Department of Electrical Engineering, Indian Institute of Science, Bangalore-560 012
e-mail: kasi@ee.iisc.ernet.in, anoopkp@ee.iisc.ernet.in

Abstract

With the introduction of 2D flat-panel X-ray detectors, 3D image reconstruction using helical cone-beam tomography is fast replacing the conventional 2D reconstruction techniques. In 3D image reconstruction, the source orbit or scanning geometry should satisfy the data sufficiency or completeness condition for exact reconstruction. The helical scan geometry satisfies this condition and hence can give exact reconstruction. The theoretically exact helical cone-beam reconstruction algorithm proposed by Katsevich is a breakthrough and has attracted interest in the 3D reconstruction using helical cone-beam Computed Tomography.

In many practical situations, the available projection data is incomplete. One such case is where the detector plane does not completely cover the full extent of the object being imaged in lateral direction resulting in truncated projections. This result in artifacts that mask small features near to the periphery of the ROI when reconstructed using the convolution back projection (CBP) method assuming that the projection data is complete. A number of techniques exist which deal with completion of missing data followed by the CBP reconstruction. In 2D, linear prediction (LP) extrapolation has been shown to be efficient for data completion, involving minimal assumptions on the nature of the data, producing smooth extensions of the missing projection data.

In this paper, we propose to extend the LP approach for extrapolating helical cone beam truncated data. The projection on the multi row flat panel detectors has missing columns towards either ends in the lateral direction in truncated data situation. The available data from each detector row is modeled using a linear predictor. The available data is extrapolated and this completed projection data is backprojected using the Katsevich algorithm. Simulation results show the efficacy of the proposed method.

Keywords: *Helical cone beam tomography, Truncated data, Katsevich Algorithm, linear prediction*

1. Introduction

With the introduction of multi-row and flat panel X-ray detectors in Computed Tomography (CT) scanners, helical cone-beam reconstruction has become an important subject of research in x-ray computed tomography. The helical scan CT scanner has decreased scanning time and increased x-ray source utilization. For exact 3D reconstruction, the Tuy-Smith data completeness condition is stated as "*A necessary condition for exact reconstruction is that for every plane that intersects the*

object there exists at least one cone-beam source point". The helical geometry satisfies this condition and hence can give exact reconstruction.

In many practical imaging situations, the projection data available is incomplete. In general, there are four types of incompleteness that arises in CT- truncated, hollow, arbitrary missing and limited angle projection data. In helical scan CT, the first three types of incomplete projection data problems are relevant. Iterative reconstruction techniques in CT provide a solution to reconstruction with sparse/incomplete projection data. These techniques include methods like ART and Statistical Inversion. However they are computationally expensive.

The most popular convolution back projection (CBP) algorithm requires complete projection data and does not work well when applied with sparse/incomplete projections. A number of projection completion techniques, followed by the fast and efficient CBP reconstruction algorithm for reconstruction, have been proposed for different incomplete projection data problems. In 2D, projection completion using linear prediction (LP) [1] has been shown to be efficient for all the incomplete data situations. In this paper, we extend the LP approach for projection completion to the helical scan truncated projection data.

2. 3D Radon Transform and Inverse

The three dimensional Radon transform of a function $f(\boldsymbol{x})$ consists of plane integrals taken over all planes in 3D. The transform is given by

$$\Re f(\rho\bar{\xi}) = \int_{-\infty}^{\infty}\int_{-\infty}^{\infty}\int_{-\infty}^{\infty} f(\bar{x})\delta(\bar{x}.\bar{\xi} - \rho)d\bar{x} \qquad (1)$$

where, $\bar{x} = (x, y, z)$ is a vector, $\bar{\xi} = (\sin\theta\cos\varphi, \sin\theta\sin\varphi, \cos\theta)$ is a unit vector perpendicular to the plane of integration, $\boldsymbol{\rho}$ is the distance of the plane from the origin and $\bar{x}.\bar{\xi} = \rho$ represents a plane of integration in 3D. The inversion formula [2] for the 3D Radon transform is given by

$$f(\bar{x}) = \frac{-1}{8\pi^2}\int_{\theta=\frac{-\pi}{2}}^{\frac{\pi}{2}}\int_{\varphi=0}^{2\pi}\frac{\partial^2}{\partial\rho^2}\Re f((\bar{x}.\bar{\xi})\bar{\xi})\sin\theta\, d\varphi\, d\theta$$

. (2)

The Cone Beam Transform $D_f(\mathbf{y}, \beta)$ of f is given by

$$D_f(y,\beta) \equiv \int_0^{\infty} f(y + t\beta)\, dt \quad , \qquad \beta \in S^2 \quad . \qquad (3)$$

The cone beam transform computes the line integral along a semi-infinite line starting from point $\boldsymbol{y}$ and pointing along the direction given by the vector $\boldsymbol{\beta}$. This transform comes up in helical cone-beam tomography and its relation with the 3D Radon is used to arrive at inversion formulas.

Numerous algorithms have been suggested till date for inversion of helical cone beam transform. The major ones are the FDK-like algorithms which are extensions of the FDK method used for circular cone-beam reconstruction [3], the rebinning algorithms [4], the PHI method of Schaller *et al* [5] which are exact but more demanding in terms of computations and memory and Katsevich's Algorithm [6] which is both exact and efficient. The FDK method, rebinning and the methods based on extensions of Grangeat's theory, involves approximations and are not exact algorithms. We consider only the exact and efficient Katsevich algorithm for reconstruction after the projection completion.

2.1. Katsevich Algorithm for 3D Reconstruction

An exact solution to the image reconstruction problem from axially truncated cone-beam projections has been recently introduced by Katsevich [6] and it can be implemented in an efficient filtered-backprojection (FBP) fashion.

In this algorithm, the CB projections are first differentiated with respect to the helical path length; a 1D Hilbert filter is then applied along one or several families of straight lines in the detector, and the filtered CB projections are finally backprojected.

The main result of the improved exact filtered backprojection algorithm suggested by Katsevich is the following [6]:

For $f \in C_0^\infty(\mathbf{U})$ one has

$$f(\mathbf{x}) := -\frac{1}{2\pi^2}\int_{I_{PI}(\mathbf{x})} \frac{1}{|\mathbf{x}-\mathbf{y}(s)|}\Psi(s,\boldsymbol{\beta}(s,\mathbf{x}))\,ds \tag{4}$$

where,

$$\Psi(s,\boldsymbol{\beta}) := \int_0^{2\pi} \frac{\partial}{\partial q} D_f(\mathbf{y}(q),(\cos(\theta+\gamma),\sin(\theta+\gamma)))\Big|_{q=s} \frac{1}{\sin\gamma}\,d\gamma, \boldsymbol{\beta} \in \prod(s_2) \tag{5}$$

Equation (5) is of convolution type and one application of Fourier transfrom gives values $\Psi(s,\boldsymbol{\beta})$ of for all $\boldsymbol{\beta} \in \prod(s_2)$ at one. The above equations are hence in the filtered backprojection form, where (2) gives a shift-invariant filtering of the derivative of the cone-beam data $D_f(\mathbf{y}(s),\beta)$ and (1) performs backprojection to give the reconstructed object function $f(\boldsymbol{x})$.

2.2. Implementation for Flat Panel Detectors

The Katsevich's formulation of the algorithm applies for generalized detector geometry. Wang et. al. [7] recently suggested a formulation of the Katsevich's algorithm for the special case of planar detector geometry.

The helical scanning locus can be defined as

$$C \equiv \left\{ \begin{array}{l} \boldsymbol{y} \in R^3 : y_1 = R\cos(s), y_2 = R\sin(s), \\ y_3 = \dfrac{sh}{2\pi}, s \in R \end{array} \right\}$$

where, $h > 0$ is the helical pitch, R the radius of the helix and s is an angular parameter which indicates the position on the spiral. Let **u** and **v** represent the horizontal and vertical axis for the detector plane. The uniformly sampled values of cone beam data $D_f(\mathbf{y}(s),\beta)$ are available for sampling intervals Δs, Δu, Δv for s, u and v as follows:

$$g(s_k, u_m, v_n), \quad 1 \le k < K, \quad |m| \le M, \quad |n| \le N$$

where, k, m, n are sampling indexes of sampling points for s, u and v. The following steps are involved in the implementation of Katsevich's algorithm

Take first order derivatives of the cone-beam data: use the two point difference formulae.

Filtration of derivative data: First re-sampling via interpolation along the direction of v. Perform a pre-weighting operation on the first derivatives of the cone-beam data and Hilbert filtering along $L(s_1)$ lines followed by post-weighting of the resulting data. Re-sample the filtered data on to cartesian grid using linear interpolation.

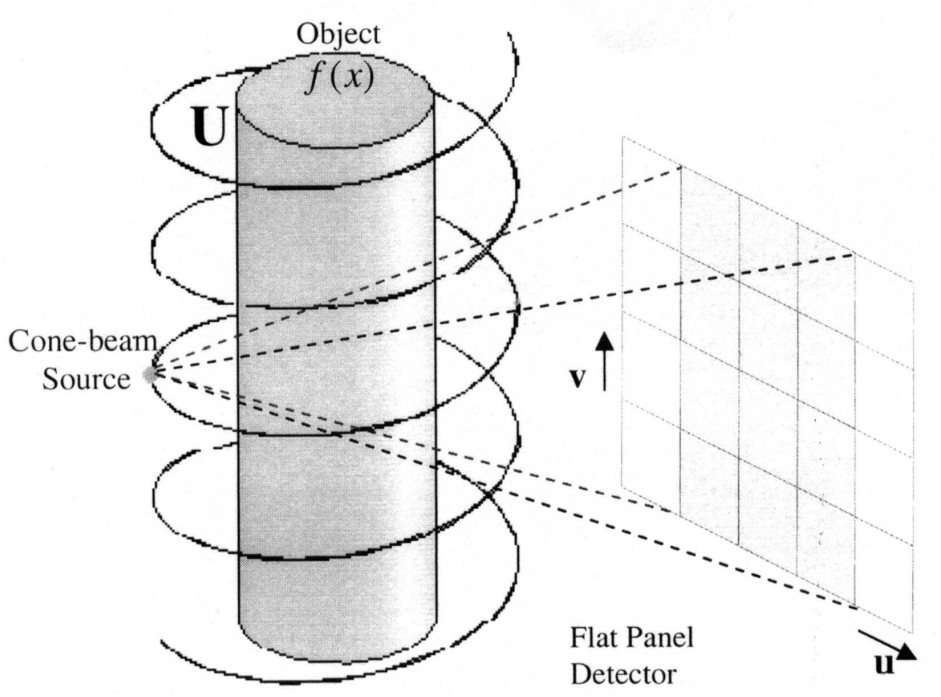

Fig. 1: Projection Truncation in 3D helical scanning

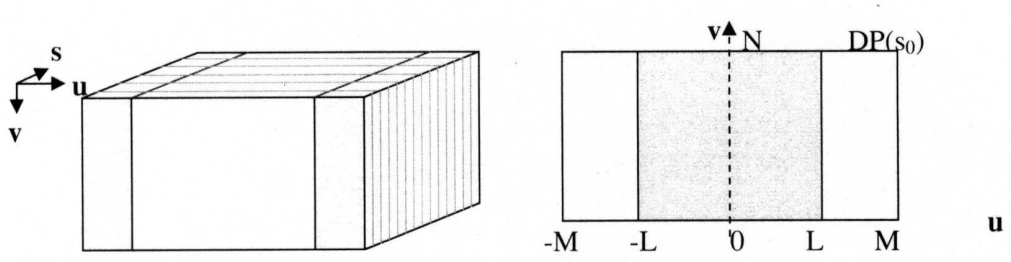

Fig. 2: (a) Projection data arranged as a stack of detector planes. The shaded region indicates region of truncation. (b) Projection data for one of the Detector planes for the source position $y(s_0)$

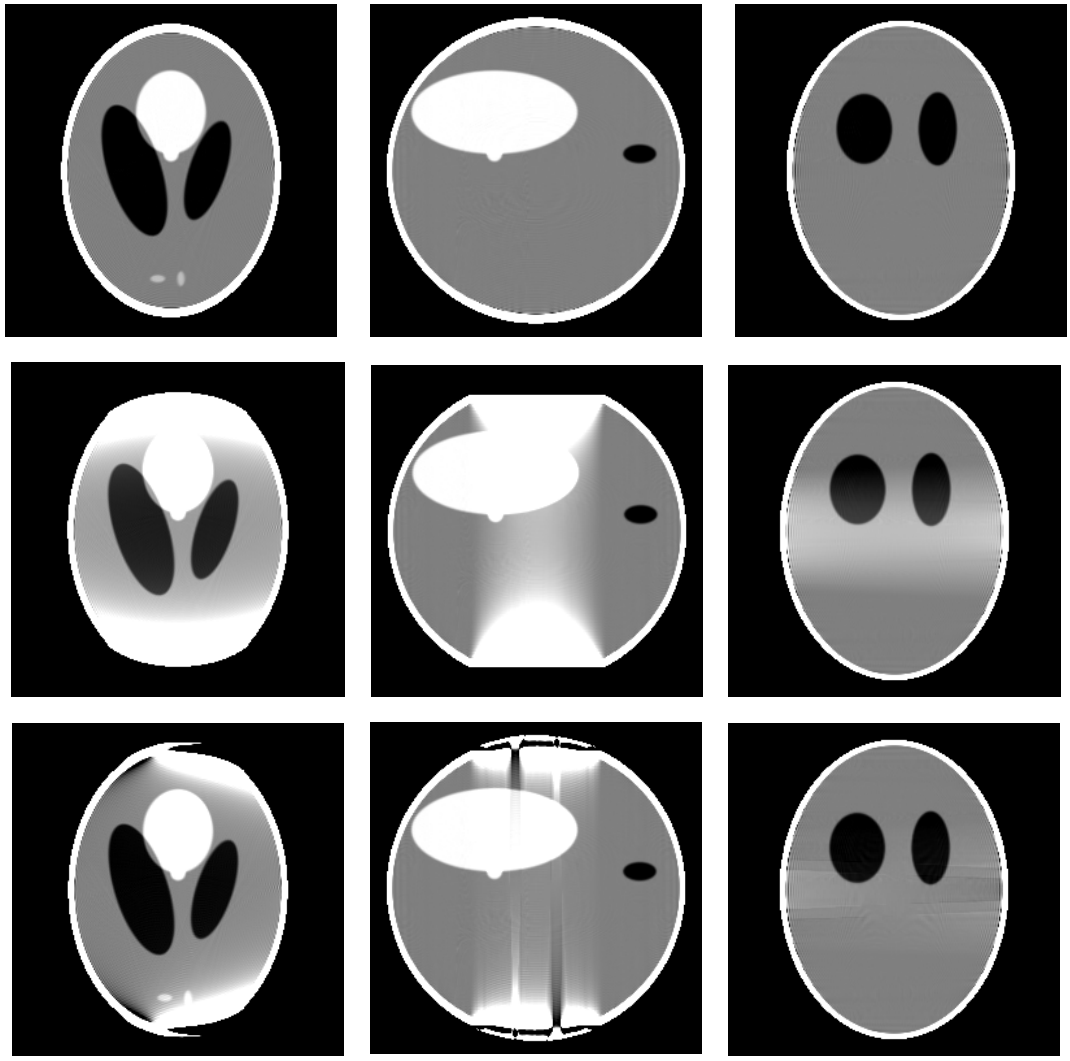

Fig. 3: Reconstruction of low contrast Shepp-Logan Phantom, 35 detectors are truncated in the detector plane on either side. The first row - complete projection data, the second row - truncated projection data and the third row - projection completion using linear prediction. Left column shows the slice at z = -0.25, the middle shows slice at y = 0 and right column shows slice at x = 0. The gray scale window used is [1.0 1.04].

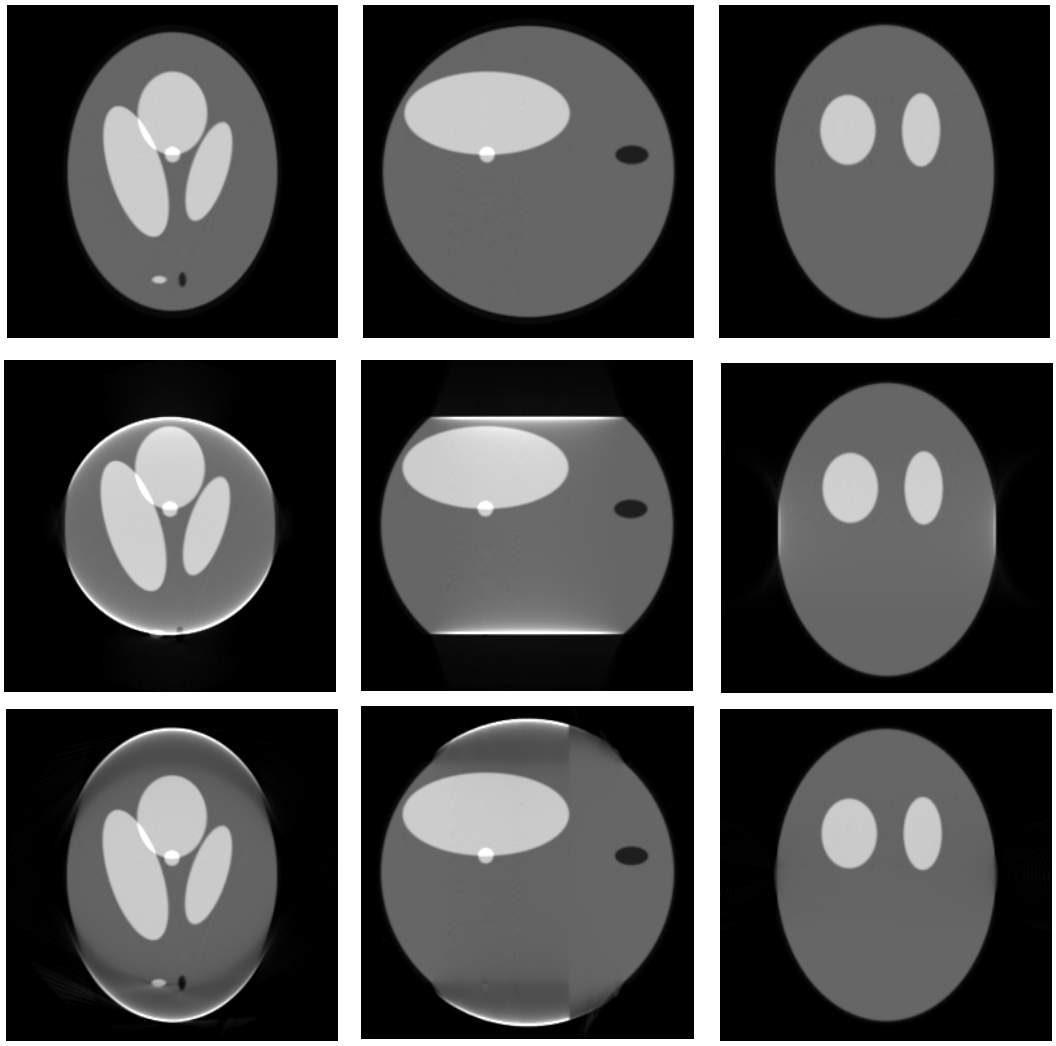

Fig. 4: Reconstruction of high contrast Shepp-Logan Phantom, 55 detectors are truncated in the detector plane on either side. The first row - complete projection data, the second row - truncated projection data and the third row - projection completion using linear prediction. Left column shows the slice at z = -0.25, the middle shows slice at y = 0 and right column shows slice at x = 0. The gray scale window used is [0.0 2.5]

Back project the filtered data. This backprojection is similar to the backprojection in the FDK method [3].

The relevant details pertaining to the discreet implementation can be found in [7].

3. Truncated Projection Data

Truncated projection data occurs in many practical situations. An example of this is when the object has larger dimension than the field of view of the imaging system. Another example is the Region of Interest scans where usually a restricted region scan is performed. Such situations are also referred to as limited field of view or as restricted region scans.

The 3D cone-beam projection data consists of multiple projections measured on the 2D detector plane. For each position $y(s)$ on the spiral we get a two dimensional projection data. Truncation of 3D projection data can happen in two possible ways – in lateral direction or along axial direction. The truncation in axial direction is referred to as "Long object problem". This problem is solved by Katsevich's algorithm. The projection data truncation considered here is in the lateral truncation as shown in Fig.1.

The projection data collected can be viewed as a stack of detector plane data, each plane corresponding to a particular source position on the spiral. This is shown in Fig.2, where each of the *u*-*v* planes is a detector plane. *s* denotes the angular parameter of the spiral. The projection data collected can be viewed as a stack of detector plane data, each plane corresponding to a particular source position on the spiral. This is shown in Fig.2, where each of the *u*-*v* planes is a detector plane. *s* denotes the angular parameter of the spiral locus *C*.

4. Projection Completion using Linear Prediction

Linear Prediction (LP) is one of the most powerful approaches for parametric modeling of a stationary random signal. In LP, a given signal is modeled as the output of a causal and stable time invariant linear system excited by an unknown signal (white noise process). The LP models are characterized by the model order and the model parameters.

The most widely used model for a signal $s(n)$ is autoregressive $AR(p)$ or all-pole model [8]. Choosing an LP model for a signal requires estimation of the model order and estimation of the model parameters. The $AR(p)$ model parameters can be obtained by solving a linear system of equations. Hence AR modeling is simpler, inexpensive and computationally less complex compared to autoregressive moving average (ARMA) and moving average (MA) modeling.

The input out relationship for an $AR(p)$ is given by,

$$s(n) = -\sum_{k=1}^{p} a_k s(n-k) + Gu(n) \qquad (6)$$

Therefore, $s(n)$ is a linear function of the past outputs and the present input. The first term, $\hat{s}(n) \equiv -\sum_{k=1}^{p} a_k s(n-k)$ is referred to as predicted value of $s(n)$ and the second term $u(n)$ is referred to as prediction error or residual. During modeling of a given signal, we have control over the parameters in the first term and they have to be selected so that the effect of second term is minimized.

The model order represents the number of parameters in the model. The most generally used criteria for model order

determination is the Akaike's criteria (Final Prediction Error Criteria and Akaike Information Criteria). Once the order of the model is selected, different AR parameter estimation techniques are available. The popular ones are a using Levinson-Durbin recursion to solve the Yule-Walker equations, Burg's constrained least-square estimation algorithm and Marple's unconstrained least-square estimation procedure.

The AR model for a signal $s(n)$ gives a one-step predictor. The parameters $\{a_p(k)\}_{k=1}^{p}$ once estimated, gives us the prediction filter $\hat{s}(n)$ which will be the best linear mean-square predictor of $s(n)$ based on its previous p samples. Thus, given the past values $s(n-p),...,s(n-2),s(n-1)$ the current value $s(n)$ is linearly predicted using the filter given in (4). This filter is called a one-step *forward linear predictor*. Similarly, if the data sequence $s(n),s(n-1),...,s(n-p+1)$ is available and we wish to predict the value $s(n-p)$ we employ a one-step *backward linear predictor* of same order p:

$$\hat{s}(n-p) = -\sum_{k=0}^{p-1} b_p(k)\, s(n-k) \qquad (7)$$

where the weighting coefficients of the backward predictor $b_p(k) = a_p^*(p-k)$, $k = 0,1,...,p$ and $a_0 = 1$.

Though the AR model yields a one-step predictor, we can consider the predicted values as part of the original data sequence and continue extrapolation for the next sample. Such an approach is often adopted for prediction and forecasting applications. Such an approach has been shown to be equivalent to maximum entropy extension of the signal. Thus this method involves the least amount of assumptions on the form of the original signal.

4.1 Data Completion using Linear Prediction

For truncated projections, the cone-beam projection data measured over planar detectors $g(s,u,v)$, are available only for a limited range of u values. For a particular source position, say $y(s_0)$, the projection data available on the detector plane is shown below in Fig. 2.

Let sampled data matrix corresponding to complete projection data be $\mathbf{G} = \{g(s_k, i\Delta u, j\Delta v)\}$, $1 \le k \le K$, $i \le |M|$, $j \le |N|$. Therefore the data matrix corresponding to the truncation shown in Fig. 6 will be $\boldsymbol{G}_T = \{g(s_k, i\Delta u, j\Delta v)\}$, $1 \le k \le K$, $i \le |L|$, $j \le |N|$.

For a particular source position, each row of the detector can be thought of as a one dimensional signal - $\{g_{k,j}(i)\}$ and linear prediction can be used to extrapolate the signal in the range $L < |i| \le M$. $\{g_{k,j}(i)\}$ is modeled as an *AR*(*p*) process.

$$\hat{g}_{k,j}(i) = -\sum_{l=1}^{p} a(l)\, g_{k,j}(i-l) \qquad (8)$$

The available data is used to fit an *AR*(*p*) process. The missing data between $L < i \le M$ is extrapolated using forward linear prediction and between $-M \le i < -L$ is extrapolated using backward predictor implemented as given in (7). This completion process can be carried out for all detector rows, for all source positions. The completed projections can be passed to the Katsevich's algorithm.

5. Simulation Results

The simulations were carried out on three different phantoms. The first is the low contrast 3D shepp-logan head phantom: a set of 10 overlapping ellipses as defined [9].The second phantom is a High contrast version of the shepp-logan given in [10]. The third phantom is taken from [1]. The

imaging parameters used for simulation of Katsevich algorithm are given in Table 1.

Truncated projection data is obtained by removing 30 and 55 detectors on either side in the detector plane as shown in Fig. 2 for the low and high contrast phantoms respectively. An *AR*(5) model was found to be sufficient for modeling the cone beam projection data of the Shepp-logan phantom. The Burg's method was used for estimation of the AR parameters. The truncated detector values are predicted using the AR model only up to the boundary of the object using a priori knowledge of the phantom. We impose the non-negativity constraint on the completed projection data.

Table 1: Imaging Parameters

Cone-beam imaging parameters used in the numerical simulation	
Scanning Radius (R)	75 cm
Source to detector distance (D)	150 cm
Helical pitch (h)	12.5 cm
Object radius (r)	25 cm
Number of projections per turn	750
Scanning range (K = 1536)	$s \varepsilon [-4\pi , 4\pi]$
Detector size	300 x 40
Number of lines $L(s_l)$ per projection (Q = 64)	128
Reconstruction matrix	256 x 256x 256

The results obtained in the simulation are shown in Fig. (3) and (4). It is seen that the two small ellipses at bottom in column one in Fig. 3 and 4 were recovered using the proposed algorithm and the high contrast artifacts have been reduced considerably.

6. Conclusion

A linear prediction approach to completion of 3D helical cone-beam projection data was discussed. The method required no a priori knowledge about the shape or extent of the object. Simulation results show the validity of such an approach. Features which were not visible in the reconstruction of truncated data were recovered by this method.

7. References

1. K. Rajgopal, N. Srinivasa, and K.R. Ramakrishnan, "Image reconstruction from incomplete projection data: A linear prediction approach." *Medical Imaging Systems, Techniques and Applications: Modalities*, Gordon and Breach International Series in Engineering, Technology and Applied Science, 281-328, 1997.
2. Natterer F., "*The Mathematics of Computerized Tomography*", Classics in Applied Mathematics 32, SIAM, 1986.
3. Feldkamp L A, Davis L C and Kress J W, "Practical cone-beam algorithm" *J. Opt. Soc. Am.* A **6** 612–619, 1984
4. Kachelriess M, Schaller S and Kalender W A "Advanced single-slice rebinning in cone-beam spiral CT", *Med. Phys.* **27** 754–772, 2000
5. Schaller S, Noo F, Sauer F, Tam K C, Lauritsch G and Flohr T "Exact Radon rebinning algorithm for the long object problem in helical cone-beam CT", *IEEE Trans. Med. Imaging* **19** 361–375, 2000
6. A. Katsevich, "An improved exact filtered backprojection algorithm for spiral computed tomography", *Adv. Appl. Math.*, **32**, 681-697, 2004.
7. Ge Wang, Hengyong Yu, "Studies on Implementation of the Katsevich algorithm for spiral cone-beam CT", *J. X-ray Science and Tech.*, **12**, 97-116, IOS Press, 2004.
8. J. Makhoul, "Linear prediction: A tutorial review", *Proc. IEEE*, **63,** 561-580, 1975.
9. A. C. Kak, Malcolm Slaney, "*Principles of Computerized Tomographic Imaging,"* Society of Industrial and Applied Mathematics, 2001.
10. H. Kudo, N. Miyagi, T. Saito, A new approach to cone-beam reconstruction without Radon transform", *Nuclear Science Symposium*, *IEEE conference record*, **3**, 1636-1643, 1998.